Scientific Research Publishing

Journal of Electromagnetic Analysis and Applications, 2026, 18(8), 141-152
https://www.scirp.org/journal/jemaa
ISSN Online: 1942-0749
ISSN Print: 1942-0730

Analytical Stability and Spectral Properties of the SVS-Based EFIE Solver for Electromagnetic Scattering Analysis

Osman Goni

Department of Electrical and Electronic Engineering, Bangladesh Army University of Engineering and Technology, Natore, Bangladesh
Email: osman.goni@bauet.ac.bd

How to cite this paper: Goni, O. (2026) Analytical Stability and Spectral Properties of the SVS-Based EFIE Solver for Electromagnetic Scattering Analysis. *Journal of Electromagnetic Analysis and Applications*, **18**, 141-152.
https://doi.org/10.4236/jemaa.2026.188008

Received: May 21, 2026
Accepted: August 28, 2026
Published: August 31, 2026

Abstract

This paper presents a Surface-Volume-Surface (SVS) EFIE formulation that integrates surface and volume integral representations to improve the accuracy and stability of electromagnetic field computation in composite structures. The exact solution of the Surface-Volume-Surface Electric Field Integral Equation (SVS-EFIE) is presented for both electric current (J-type and magnetic current based or M-type) formulations for the problem of radiation and scattering in the vicinity of homogeneous dielectric sphere. The SVS framework enhances field continuity across interfaces and reduces numerical errors associated with conventional EFIE implementations, particularly in near-field and multi-region scenarios. The formulation is implemented using the Method of Moments (MoM) with appropriate basis and testing functions to ensure numerical stability and convergence. It also reveals the spectral properties of its individual operators. The MoM impedance matrix features bounded condition number with increasing order of discretization, similar with analogous exact MoM solution of the surface EFIE on Perfectly Electrically Conducting (PEC) sphere. It also shows that SVS-EFIE-J formulation tends to infinity at low frequency and suffers from low-frequency breakdown issue, likewise regular EFIE. However, with SVS-EFIE-M, the formulation is stable at low frequency. Also, this work suggests that with SVS-EFIE-M, the spectral behavior is almost constant after a certain range of the discretization order.

Keywords

Electric Field Integral Equations, Single-Source, Surface-Volume-Surface, Volume Equivalence Principle, Method of Moments (MoM)

1. Introduction

Accurate analysis of electromagnetic scattering and radiation is essential for the design and optimization of modern communication and sensing systems, including antennas, radar platforms, and Electromagnetic Compatibility (EMC) solutions. Among various numerical techniques, the Electric Field Integral Equation (EFIE) has been widely adopted due to its suitability for open-region problems and its compatibility with surface discretization methods such as the Method of Moments (MoM). However, conventional surface-based EFIE formulations often encounter limitations when applied to structures involving material inhomogeneities, dielectric regions, or complex multi-domain interactions. In particular, surface-only EFIE approaches may fail to accurately capture volumetric polarization effects and field continuity across interfaces, leading to reduced accuracy in near-field prediction and scattering analysis. Additionally, numerical challenges such as slow convergence and instability can arise due to the improper handling of interactions between surface and volume regions. These limitations motivate the need for a more comprehensive formulation that integrates both surface and volumetric electromagnetic behavior.

To address these challenges, this paper proposes a Surface-Volume-Surface (SVS) EFIE formulation that combines surface current representations with volume integral contributions in a unified framework. The SVS-EFIE is a type of single-source integral equation [1]-[5] which is formed by constraining of a single-source field representation with the volume equivalence principle [6] enforced on the boundary of the scatterer but only for the tangential component of the total electric field. The term "single-source" here represents as the obtained electric field integral equations via a single unknown surface current density rather than two independent physical currents. The SVS-EFIE formulation is implemented within a Method of Moments framework, employing suitable basis and testing functions to ensure numerical stability and computational efficiency. From a signal-processing perspective, the proposed method can be interpreted as a structured coupling mechanism that enhances numerical conditioning and mitigates errors arising from discontinuities and singular interactions. As a result, the approach offers improved convergence characteristics compared to conventional EFIE techniques.

In order to validate the rigorous nature of the SVS-EFIE, we performed its exact solution for a homogeneous spherical scatterer using Galerkin MoM with a complete set of orthogonal rotational and irrotational spherical functions introduced on the surface of the sphere by analogy with how the exact solution of the traditional surface EFIE (S-EFIE) and surface Magnetic Field Integral Equation (S-MFIE) was obtained for PEC sphere in [7]. Due to diagonal nature of the resultant SLAE, each coefficient in the current expansion can be expressed as the ratio of a corresponding spherical harmonic expansion coefficient in the excitation vector element and its corresponding diagonal matrix element, which are both available in either closed form or the form of 1D integrals [8]. This provides the formal exact solution for the fictitious current playing the role of the unknown function in the SVS-EFIE in the form of infinite series over rotational and irrotational sets of surface vector spherical functions. The expansion is truncated at the orders fully capturing bandwidth of the incident field and providing accuracy of the solution close to the machine precision. Upon substitution of the fictitious current solution into the single-source field representation inside the sphere, we can obtain exact expressions for the electric and magnetic field components. The latter is numerically compared to the classical Mie series solution of the radial electric dipole radiation problem in the presence of the dielectric sphere [6]. Upon sufficient number of terms retained in the MoM solution of the SVS-EFIE and Mie series, the two are shown to agree to 12 digits of accuracy, hence validating the SVS-EFIE formulation.

The effectiveness of the proposed method is demonstrated through several benchmark electromagnetic scattering problems, where it shows enhanced accuracy in field distribution and Radar Cross-Section (RCS) estimation. Owing to its improved performance and flexibility, the SVS-EFIE formulation is applicable to a wide range of practical problems in antenna design, EMC analysis, and advanced wireless communication systems.

2. Surface-Volume-Surface Electric Field Integral Equation

Given by the volume equivalence principle [6]

$$\boldsymbol{E}(\boldsymbol{r}) = \boldsymbol{E}^{inc}(\boldsymbol{r}) + k_0^2(\epsilon - 1)\int_V \overline{\boldsymbol{G}}_{e0}(\boldsymbol{r},\boldsymbol{r}')\cdot\boldsymbol{E}(\boldsymbol{r}')\mathrm{d}v',\ \ \forall\boldsymbol{r} \tag{1}$$

which produces the following well-known V-EFIE with respect to the unknown electric field inside the scatterer upon localization of the observation point to the volume of the scatterer

$$\boldsymbol{E}(\boldsymbol{r}) - k_0^2(\epsilon - 1)\int_V \overline{\boldsymbol{G}}_{e0}(\boldsymbol{r},\boldsymbol{r}')\cdot\boldsymbol{E}(\boldsymbol{r}')\mathrm{d}v' = \boldsymbol{E}^{inc}(\boldsymbol{r}),\ \ \boldsymbol{r}\in V. \tag{2}$$

Volume equivalence principle can be also used to constrain the single-source representation [4]

$$\begin{aligned}\boldsymbol{E}(\boldsymbol{r}') = {} & i\omega\mu_0\int_S \overline{\overline{\boldsymbol{G}}}_{e\epsilon}(\boldsymbol{r}',\boldsymbol{r}'')\cdot a\boldsymbol{J}(\boldsymbol{r}'')\mathrm{d}s'' \\ & -\int_S \overline{\boldsymbol{G}}_{m\epsilon}(\boldsymbol{r}',\boldsymbol{r}'')\cdot b\hat{\boldsymbol{n}}''\times\boldsymbol{J}(\boldsymbol{r}'')\mathrm{d}s'',\ \ \boldsymbol{r}'\in V,\end{aligned} \tag{3}$$

where $\boldsymbol{J}$ is the fictitious electric current density, a and b are arbitrary constants, ω is the cyclic frequency of the time harmonic field under time convention $\mathrm{e}^{i\omega t}$, which is suppressed here and throughout the paper. To produce the integral equation with respect to the fictitious surface current density $\boldsymbol{J}(\boldsymbol{r}')$. For that purpose, we substitute (3) into (2) and enforce the latter for the tangential component of the electric field as we tend the observation point $\boldsymbol{r}$ to the boundary S from the inside

$$
\begin{aligned}
&-i\omega\mu_0\hat{\boldsymbol{n}}\times\int_S \bar{\boldsymbol{G}}_{e\epsilon}\left(\boldsymbol{r},\boldsymbol{r}''\right)\cdot a\boldsymbol{J}\left(\boldsymbol{r}''\right)\mathrm{d}s''+\hat{\boldsymbol{n}}\times\int_S \bar{\boldsymbol{G}}_{m\epsilon}\left(\boldsymbol{r},\boldsymbol{r}''\right)\cdot b\hat{\boldsymbol{n}}''\times\boldsymbol{J}\left(\boldsymbol{r}''\right)\mathrm{d}s'' \\
&-k_0^2\left(\epsilon-1\right)\hat{\boldsymbol{n}}\times\int_V \bar{\boldsymbol{G}}_{e0}\left(\boldsymbol{r},\boldsymbol{r}'\right)\cdot\left\{-i\omega\mu_0\int_S \bar{\boldsymbol{G}}_{e\epsilon}\left(\boldsymbol{r}',\boldsymbol{r}''\right)\cdot a\boldsymbol{J}\left(\boldsymbol{r}''\right)\mathrm{d}s''\right. \\
&\left.+\int_S \bar{\boldsymbol{G}}_{m\epsilon}\left(\boldsymbol{r}',\boldsymbol{r}''\right)\cdot b\hat{\boldsymbol{n}}''\times\boldsymbol{J}\left(\boldsymbol{r}''\right)\mathrm{d}s''\right\}\mathrm{d}v'=\hat{\boldsymbol{n}}\times\boldsymbol{E}^{inc}\left(\boldsymbol{r}\right),\ \ \boldsymbol{r}\in V,\ \ \boldsymbol{r}\to S.
\end{aligned}
\tag{4}
$$

The above integral equation is the Combined-Source SVS-EFIE (CS-SVS-EFIE) with respect to the unknown current $\boldsymbol{J}$. Here, the "combined-source" is a formulation combining electric and magnetic single-source representations, scaled by parameters a and b to improve robustness. In its complete form (4), it was hypothesized in [4]. To produce the integral equation with respect to the fictitious surface current density $\boldsymbol{J}\left(\boldsymbol{r}''\right)$, we substitute (3) with particular case of $a=1$ and $b=0$ into (2) and enforce the latter for the tangential component of the electric field as we tend the observation point $\boldsymbol{r}$ to the boundary S from the inside

$$
\begin{aligned}
&i\omega\mu_0\hat{\boldsymbol{n}}\times\int_S \bar{\bar{\boldsymbol{G}}}_{e\epsilon}\left(\boldsymbol{r},\boldsymbol{r}''\right)\cdot\boldsymbol{J}\left(\boldsymbol{r}''\right)\mathrm{d}s'' \\
&+i\omega\mu_0 k_0^2\left(\epsilon-1\right)\hat{\boldsymbol{n}}\times\int_V \bar{\bar{\boldsymbol{G}}}_{e0}\left(\boldsymbol{r},\boldsymbol{r}'\right)\cdot\int_S \bar{\bar{\boldsymbol{G}}}_{e\epsilon}\left(\boldsymbol{r}',\boldsymbol{r}''\right)\cdot\boldsymbol{J}\left(\boldsymbol{r}''\right)\mathrm{d}s''\mathrm{d}v' \\
&=\hat{\boldsymbol{n}}\times\boldsymbol{E}^{inc}\left(\boldsymbol{r}\right),\ \ \boldsymbol{r}\in S.
\end{aligned}
\tag{5}
$$

It has been shown that the SVS-EFIE can also be formulated in terms of $\boldsymbol{M}$. Where $\boldsymbol{M}$ is the fictitious magnetic current density. In that case, CS-SVS-EFIE can be written in terms of current $\boldsymbol{M}=\hat{\boldsymbol{n}}\times\boldsymbol{J}$ by considering $a=0$ and $b=1$ and hence we call SVS-EFIE-M formulation

$$
\begin{aligned}
&\hat{\boldsymbol{n}}\times\int_S \bar{\boldsymbol{G}}_{m\epsilon}\left(\boldsymbol{r},\boldsymbol{r}''\right)\cdot\hat{\boldsymbol{n}}\times\boldsymbol{J}\left(\boldsymbol{r}''\right)\mathrm{d}s'' \\
&-k_0^2\left(\epsilon-1\right)\hat{\boldsymbol{n}}\times\int_V \bar{\boldsymbol{G}}_{e0}\left(\boldsymbol{r},\boldsymbol{r}'\right)\int_S \bar{\boldsymbol{G}}_{m\epsilon}\left(\boldsymbol{r}',\boldsymbol{r}''\right)\cdot\hat{\boldsymbol{n}}\times\boldsymbol{J}\left(\boldsymbol{r}''\right)\mathrm{d}s''\mathrm{d}v' \\
&=\hat{\boldsymbol{n}}\times\boldsymbol{E}^{inc}\left(\boldsymbol{r}\right),\ \ \boldsymbol{r}\in S,
\end{aligned}
\tag{6}
$$

The SVS-EFIE-J (5) can also be represented as the following operator form

$$
\mathcal{T}_{e\epsilon}^{S,S}\circ\boldsymbol{J}+\mathcal{T}_{e0}^{S,V}\circ\mathcal{T}_{e\epsilon}^{V,S}\circ\boldsymbol{J}=\hat{\boldsymbol{n}}\times\boldsymbol{E}^{inc}\left(\boldsymbol{r}\right),\ \ \boldsymbol{r}\in S,
\tag{7}
$$

where the operators are defined, as follows:

$$
\mathcal{T}_{e\epsilon}^{S,S}\circ\boldsymbol{J}=i\omega\mu_0\hat{\boldsymbol{n}}\times\int_S \bar{\bar{\boldsymbol{G}}}_{e\epsilon}\left(\boldsymbol{r},\boldsymbol{r}''\right)\cdot\boldsymbol{J}\left(\boldsymbol{r}''\right)\mathrm{d}s'',\ \ \boldsymbol{r}\in S,
\tag{8}
$$

$$
\mathcal{T}_{e\epsilon}^{V,S}\circ\boldsymbol{J}=i\omega\mu_0\int_S \bar{\bar{\boldsymbol{G}}}_{e\epsilon}\left(\boldsymbol{r}',\boldsymbol{r}''\right)\cdot\boldsymbol{J}\left(\boldsymbol{r}''\right)\mathrm{d}s'',\ \ \boldsymbol{r}'\in V,
\tag{9}
$$

$$
\mathcal{T}_{e0}^{S,V}\circ\boldsymbol{i}=k_0^2\left(\epsilon-1\right)\hat{\boldsymbol{n}}\times\int_V \bar{\bar{\boldsymbol{G}}}_{e0}\left(\boldsymbol{r},\boldsymbol{r}'\right)\cdot\boldsymbol{i}\left(\boldsymbol{r}'\right)\mathrm{d}v',\ \ \boldsymbol{r}\in S.
\tag{10}
$$

Conveniently, the above SVS-EFIE-M (6) can also be represented as the following compact operator form

$$
\mathcal{T}_{m\epsilon}^{S,S}\circ\boldsymbol{M}-\mathcal{T}_{e0}^{S,V}\circ\mathcal{T}_{m\epsilon}^{V,S}\circ\boldsymbol{M}=\hat{\boldsymbol{n}}\times\boldsymbol{E}^{inc}\left(\boldsymbol{r}\right),\ \ \boldsymbol{r}\in S.
\tag{11}
$$

Here, the integral operators are defined, as follows:

$$\mathcal{T}_{m\epsilon}^{S,S} \circ \boldsymbol{M} = \hat{\boldsymbol{n}} \times \int_S \overline{\overline{\boldsymbol{G}}}_{m\epsilon}\left(\boldsymbol{r},\boldsymbol{r}''\right) \cdot \boldsymbol{M}\left(\boldsymbol{r}''\right) \mathrm{d}s'', \ \ \boldsymbol{r} \in S, \tag{12}$$

$$\mathcal{T}_{m\epsilon}^{V,S} \circ \boldsymbol{M} = \int_S \overline{\overline{\boldsymbol{G}}}_{m\epsilon}\left(\boldsymbol{r}',\boldsymbol{r}''\right) \cdot \boldsymbol{M}\left(\boldsymbol{r}''\right) \mathrm{d}s'', \ \ \boldsymbol{r}' \in V, \tag{13}$$

$$\mathcal{T}_{e0}^{S,V} \circ \boldsymbol{i} = k_0^2\left(\epsilon - 1\right) \hat{\boldsymbol{n}} \times \int_V \overline{\overline{\boldsymbol{G}}}_{e0}\left(\boldsymbol{r},\boldsymbol{r}'\right) \cdot \boldsymbol{i}\left(\boldsymbol{r}'\right) \mathrm{d}v', \ \ \boldsymbol{r} \in S. \tag{14}$$

3. Exact Solution of SVS-EFIE with Galerkin MoM on Sphere

Expansion of Electric Field Dyadic Green's Function over Vector Spherical Functions

Expansion of current over spherical basis functions is reported in detail in the previous work [9] [10]. The magnetic field dyadic Green's function of homogenous medium with wavenumber k can be expanded over vector spherical functions $\boldsymbol{p}$ and $\boldsymbol{q}$, as [11] or (68) in [7]:

$$\overline{\boldsymbol{G}}_m\left(\boldsymbol{r},\boldsymbol{r}'\right) = \nabla \times \boldsymbol{G}_{e\epsilon} = -ik^2 \sum_{n,m} d_{nm}$$

$$\begin{cases} \boldsymbol{p}_{nm}^{(1)}\left(\boldsymbol{r}\right)\boldsymbol{q}_{n,-m}^{(2)}\left(\boldsymbol{r}'\right) + \boldsymbol{q}_{nm}^{(1)}\left(\boldsymbol{r}\right)p_{n,-m}^{(2)}\left(\boldsymbol{r}'\right), \left|\boldsymbol{r}\right| < \left|\boldsymbol{r}'\right|, \\ \boldsymbol{p}_{nm}^{(2)}\left(\boldsymbol{r}\right)\boldsymbol{q}_{n,-m}^{(1)}\left(\boldsymbol{r}'\right) + \boldsymbol{q}_{nm}^{(2)}\left(\boldsymbol{r}\right)p_{n,-m}^{(1)}\left(\boldsymbol{r}'\right), \left|\boldsymbol{r}\right| > \left|\boldsymbol{r}'\right|. \end{cases} \tag{15}$$

When $\left|\boldsymbol{r}\right| = \left|\boldsymbol{r}'\right|$, the average of the two above representations is taken.

4. MoM Matrix Assembly

As a result of the MoM discretization of the integral operators $\mathcal{T}_{m\epsilon}^{S,S}$, $\mathcal{T}_{m\epsilon}^{V,S}$, $\mathcal{T}_{e0}^{S,V}$ and the incident field, the SVS-EFIE (6) is reduced to the system of linear algebraic equations with respect to the vector of unknown coefficients b_{nm} and c_{nm} in the expansion of the auxiliary single source surface current density, $\boldsymbol{M} = \hat{\boldsymbol{n}} \times \boldsymbol{J}$ that has the compact representation as in (54) of [10]

$$\mathcal{Z}_{\mathrm{SVS}} \cdot \boldsymbol{I} = \boldsymbol{E}, \tag{16}$$

and $\mathcal{Z}_{\mathrm{SVS}}$ is the diagonal matrix defined as

$$\begin{aligned} \mathcal{Z}_{\mathrm{SVS}} &= \begin{bmatrix} 0 & \mathcal{Z}_{\mathrm{SVS}}^1 \\ \mathcal{Z}_{\mathrm{SVS}}^2 & 0 \end{bmatrix} \\ &= \begin{bmatrix} 0 & \mathcal{Z}_{m\epsilon}^{S_1,S_2} \\ \mathcal{Z}_{m\epsilon}^{S_2,S_1} & 0 \end{bmatrix} + \begin{bmatrix} \mathcal{Z}_{e0}^{S_1,V_1} & 0 \\ 0 & \mathcal{Z}_{e0}^{S_2,V_2} \end{bmatrix} \cdot \begin{bmatrix} \boldsymbol{\Gamma}_1 & 0 \\ 0 & \boldsymbol{\Gamma}_2 \end{bmatrix}^{-1} \cdot \begin{bmatrix} 0 & \mathcal{Z}_{m\epsilon}^{V_1,S_2} \\ \mathcal{Z}_{m\epsilon}^{V_2,S_1} & 0 \end{bmatrix}, \end{aligned} \tag{17}$$

and the Gram matrix blocks $\boldsymbol{\Gamma}_j$ are defined as in (57) of Goni (2023) [9].

4.1. Absence of Oversampling Breakdown

The behaviour of the eigenvalues of the operators forming the SVS-EFIE-M at significant value of n can be shown to be, as follows:

$$\Lambda_n^{(1)} = \Lambda_{1,m\epsilon,n}^{S,S} + \Lambda_{1,e0,n}^{S,V} \hat{\Gamma}_{2,n}^{-1} \Lambda_{1,m\epsilon,n}^{V,S} \sim O\left(n^0\right), \tag{18}$$

$$\Lambda_n^{(2)} = \Lambda_{2,m\epsilon,n}^{S,S} + \Lambda_{2,e0,n}^{S,V} \hat{\Gamma}_{1,n}^{-1} \Lambda_{2,m\epsilon,n}^{V,S} \sim O\left(n^0\right). \tag{19}$$

That is, the eigenvalues $\Lambda_n^{(1)}$ and $\Lambda_n^{(2)}$ of the Galerkin MoM impedance matrix tend to constants. This will also be numerically demonstrated in **Figure 4** in Section 5. Hence, the condition number upon the increased order of discretization n remains constant. This means that the proposed formulation does not suffer from oversampling breakdown. This is a result of Galerkin MoM solution of the SVS-EFIE-M sought in $L^2(S)$ space by analogy with the solution of the S-MFIE [7]: as both SVS-EFIE-M and S-MFIE feature the magnetic field surface operator.

4.2. Absence of Low Frequency Breakdown

Unlike the earlier J-formulation of SVS-EFIE, its proposed M-formulation does not suffer from the low-frequency breakdown either. At low frequencies, eigenvalues can be shown to behave as

$$\Lambda_n^{(1)} \sim \omega^0, \; \Lambda_n^{(2)} \sim \omega^0, \tag{20}$$

as also shown numerically in **Figure 3**. As a result, SVS-EFIE-M is free from low-frequency breakdown formulation.

Overall, the SVS-EFIE-M formulation is inherently immune to the low-frequency and oversampling breakdowns[1] unlike its SVS-EFIE-J predecessor due to its surface-to-surface operator being in the desired form of sum of a constant operator and a compact operator and its MoM discretization being performed in the $L^{(2)}(S)$ functional space.

4.3. Internal Resonances Breakdown

At certain discrete frequencies $\omega = \omega_n^{(1)}$ when

$$\Lambda_{1,m\epsilon,n}^{S,S} = -\Lambda_{1,e0,n}^{S,V} \hat{\Gamma}_{2,n}^{-1} \Lambda_{1,m\epsilon,n}^{V,S}, \tag{21}$$

nth eigenvalue $\Lambda_n^{(1)}$ becomes zero. Similarly, nth eigenvalue $\Lambda_n^{(2)}$ becomes zero at frequencies $\omega = \omega_n^{(2)}$, when

$$\Lambda_{2,m\epsilon,n}^{S,S} = -\Lambda_{2,e0,n}^{S,V} \hat{\Gamma}_{1,n}^{-1} \Lambda_{2,m\epsilon,n}^{V,S}. \tag{22}$$

Frequencies $\omega_n^{(1)}$ and $\omega_n^{(2)}$ are not equal to each other. At each such frequency $\omega_n^{(1)}$ or $\omega_n^{(2)}$, solution of the SVS-EFIE-M (6) loses its uniqueness and experiences the internal resonance breakdown, similarly with the SVS-EFIE-J (5) formulation. Notice that these resonance frequencies $\omega_n^{(1)}$ and $\omega_n^{(2)}$ do not coincide with the resonant frequencies of the surface-to-surface operator eigenvalues $\Lambda_{1,m\epsilon,n}^{S,S}$ or $\Lambda_{2,m\epsilon,n}^{S,S}$.

Neither SVS-EFIE-J nor SVS-EFIE-M formulation eliminates spurious resonances, as tangential components of electric field vanish at the surface of the sphere due to the boundary conditions. Solutions of those two formulations result in unknown electric current $\boldsymbol{J}$ and magnetic current M at the boundary, manifest-

[1]For simply connected smooth objects.

ing PEC- and PMC-like sphere. In both formulations, tangential component of the electric field exists on the right-hand side, which produces the same *n*th resonance frequencies of the cavity at which those eigenvalues become zero. Hence, this current version of the SVS-EFIE formulations does not guarantee for the elimination of the spurious resonances even though we make linear combination of those two formulations. Exploring possibilities for elimination of these spurious resonances through the combination of different SVS-EFIE formulations will be a subject of future work.

5. Evaluation of Electric Field inside the Sphere

After determining coefficients b_{nm} and c_{nm} in the MoM expansion of the fictitious current $\hat{\boldsymbol{n}}\times\boldsymbol{J}$ on S over complete set of basis functions $\boldsymbol{u}^{(1)}$ and $\boldsymbol{u}^{(2)}$, the electric field $\boldsymbol{E}$ in the scatterer volume V can be evaluated using the single-source representation (3) under condition $a=0$ and $b=1$, *i.e.*

$$\boldsymbol{E}(\boldsymbol{r})=\int_S \overline{\boldsymbol{G}}_{m\epsilon}(\boldsymbol{r},\boldsymbol{r}')\cdot\hat{\boldsymbol{n}}\times\boldsymbol{J}(\boldsymbol{r}')\mathrm{d}s',\quad \boldsymbol{r}\in V \tag{23}$$

To evaluate the field inside the sphere according to (23), we substitute expression (15) for $\overline{\boldsymbol{G}}_{m\epsilon}$ into (23)

$$\begin{aligned}\boldsymbol{E}(\boldsymbol{r})=-ik_\epsilon^2\sum_{n,m}d_{nm}\bigg(&\boldsymbol{p}_{nm}^{(1\epsilon)}(\boldsymbol{r})\int_S\boldsymbol{q}_{n,-m}^{(2\epsilon)}(\boldsymbol{r}')\cdot\hat{\boldsymbol{n}}\times\boldsymbol{J}(\boldsymbol{r}')\mathrm{d}s'\\&+\boldsymbol{q}_{nm}^{(1\epsilon)}(\boldsymbol{r})\int_S\boldsymbol{p}_{n,-m}^{(2\epsilon)}(\boldsymbol{r}')\cdot\hat{\boldsymbol{n}}\times\boldsymbol{J}(\boldsymbol{r}')\mathrm{d}s'\bigg),\quad \boldsymbol{r}\in V.\end{aligned} \tag{24}$$

Plugging current expansion $\boldsymbol{J}$ [(17) in [10]] into field definition (24), we get

$$\begin{aligned}\boldsymbol{E}(\boldsymbol{r})=-ik_\epsilon^2\sum_{n,m}d_{nm}\bigg(&\boldsymbol{p}_{nm}^{(1\epsilon)}(\boldsymbol{r})\sum_{n'',m''}b_{n''m''}\int_S\boldsymbol{q}_{n,-m}^{(2\epsilon)}(\boldsymbol{r}')\cdot\hat{\boldsymbol{n}}\times\boldsymbol{u}_{n''m''}^{(1)}(\boldsymbol{r}')\mathrm{d}s'\\&+\boldsymbol{p}_{nm}^{(1\epsilon)}(\boldsymbol{r})\sum_{n'',m''}c_{n''m''}\int_S\boldsymbol{q}_{n,-m}^{(2\epsilon)}(\boldsymbol{r}')\cdot\hat{\boldsymbol{n}}\times\boldsymbol{u}_{n''m''}^{(2)}(\boldsymbol{r}')\mathrm{d}s'\\&+\boldsymbol{q}_{nm}^{(1\epsilon)}(\boldsymbol{r})\sum_{n'',m''}b_{n''m''}\int_S\boldsymbol{p}_{n,-m}^{(2\epsilon)}(\boldsymbol{r}')\cdot\hat{\boldsymbol{n}}\times\boldsymbol{u}_{n''m''}^{(1)}(\boldsymbol{r}')\mathrm{d}s'\\&+\boldsymbol{q}_{nm}^{(1\epsilon)}(\boldsymbol{r})\sum_{n'',m''}c_{n''m''}\int_S\boldsymbol{p}_{n,-m}^{(2\epsilon)}(\boldsymbol{r}')\cdot\hat{\boldsymbol{n}}\times\boldsymbol{u}_{n''m''}^{(2)}(\boldsymbol{r}')\mathrm{d}s'\bigg).\end{aligned} \tag{25}$$

By using orthogonality relations,

$$\begin{aligned}\boldsymbol{E}(\boldsymbol{r})=-ik_\epsilon^2\sum_{n,m}d_{nm}\bigg(&\boldsymbol{p}_{nm}^{(1\epsilon)}(\boldsymbol{r})\sum_{n'',m''}c_{n''m''}\int_S\boldsymbol{q}_{n,-m}^{(2\epsilon)}(\boldsymbol{r}')\cdot\hat{\boldsymbol{n}}\times u_{n''m''}^{(2)}(\boldsymbol{r}')\mathrm{d}s'\\&+\boldsymbol{q}_{nm}^{(1\epsilon)}(\boldsymbol{r})\sum_{n'',m''}b_{n''m''}\int_S\boldsymbol{p}_{n,-m}^{(2\epsilon)}(\boldsymbol{r}')\cdot\hat{\boldsymbol{n}}\times\boldsymbol{u}_{n''m''}^{(1)}(\boldsymbol{r}')\mathrm{d}s'\bigg).\end{aligned} \tag{26}$$

$$\begin{aligned}\boldsymbol{E}(\boldsymbol{r})=-ik_\epsilon^2\sum_{n,m}d_{nm}\bigg(&\boldsymbol{p}_{nm}^{(1\epsilon)}(\boldsymbol{r})\sum_{n'',m''}c_{n''m''}\frac{-1}{k_\epsilon}\Big[k_\epsilon a h_n^{(2)}(k_\epsilon a)\Big]'\delta_{nn''}\delta_{mm''}d_{nm}^{-1}d_{n''m''}^{1/2}\\&+\boldsymbol{q}_{nm}^{(1\epsilon)}(\boldsymbol{r})\sum_{n'',m''}b_{n''m''}\Big(-ah_n^{(2)}(k_\epsilon a)\Big)\delta_{nn''}\delta_{mm''}d_{nm}^{-1}d_{n''m''}^{1/2}\bigg).\end{aligned} \tag{27}$$

Electric Field inside Sphere Due to Tangential Electric Dipole

In the case of sphere excited by the tangential dipole situated above it, both coefficients b_{nm} and c_{nm} in (27) are non-zero. This gives the following expressions for the components of the field inside the sphere after using the expansion over functions $\boldsymbol{p}$ and $\boldsymbol{q}$ in (21) - (22) of [10] (see also [11]) and the fact that only $|m|=1$ terms survive per (100) and (102) in [10].

$$E_r = -ik_\epsilon^2 \sum_{n=1}^{\infty} \sum_{m=-1,1} d_{nm}^{1/2} b_{nm} \left(\frac{n(n+1)}{k_\epsilon r} j_n(k_\epsilon r) P_n^{|m|}(\cos\theta) \mathrm{e}^{im\phi} \right) \left[-a h_n^{(2)}(k_\epsilon a) \right], \tag{28}$$

$$\begin{aligned} E_\theta = -ik_\epsilon^2 \sum_{n=1}^{\infty} \sum_{m=-1,1} d_{nm}^{1/2} \Bigg[& b_{nm} \left(\frac{1}{k_\epsilon r} \left[k_\epsilon r j_n(k_\epsilon r) \right]' \frac{\mathrm{d}}{\mathrm{d}\theta} P_n^{|m|}(\cos\theta) \mathrm{e}^{im\phi} \right) \left[-a h_n^{(2)}(k_\epsilon a) \right] \\ & + c_{nm} \left(\frac{im}{\sin\theta} P_n^{|m|}(\cos\theta) j_n(k_\epsilon r) \mathrm{e}^{im\phi} \right) \left(\frac{-1}{k_\epsilon} \left[(k_\epsilon a) h_n^{(2)}(k_\epsilon a) \right]' \right) \Bigg], \end{aligned} \tag{29}$$

$$\begin{aligned} E_\phi = -ik_\epsilon^2 \sum_{n=1}^{\infty} \sum_{m=-1,1} d_{nm}^{1/2} \Bigg[& b_{nm} \left(\frac{im}{k_\epsilon r \sin\theta} \left[k_\epsilon r j_n(k_\epsilon r) \right]' P_n^{|m|}(\cos\theta) \mathrm{e}^{im\phi} \right) \left(-a h_n^{(2)}(k_\epsilon a) \right) \\ & + c_{nm} \left(-\frac{\mathrm{d}}{\mathrm{d}\theta} P_n^{|m|}(\cos\theta) j_n(k_\epsilon r) \mathrm{e}^{im\phi} \right) \left(\frac{-1}{k_\epsilon} \left[(k_\epsilon a) h_n^{(2)}(k_\epsilon a) \right]' \right) \Bigg]. \end{aligned} \tag{30}$$

Our numerical example is for the dielectric sphere with relative permittivity of $\epsilon = 10$ and excited with the tangential θ-directed electric dipole. In this case, both the TE_r- and TM_r-waves are produced, all components of electric field are present, and they are functions of all three spherical coordinates. The tangential electric dipole is placed on z-axis at the radial distance $r_0 = 10\ \mathrm{m}$. The frequency of analysis is 599.584916 MHz. We also demonstrate the spectral properties of the SVS-EFIE-M formulation, where the functional space $L^{(2)}(S)$ is required in MoM testing for the bounded condition number of the impedance matrix. In **Figure 1** and **Figure 2**, the eigenvalues $\Lambda_{1,2}^{S,S}$ are the product of the eigenvalues $\Lambda_{1,2}^{S,V} \Gamma_{2,1}^{-1} \Lambda_{1,2}^{V,S}$ and their weighted sum is shown under condition of the Galerkin MoM testing performed in $L^2(S)$ space. The eigenvalues depicted in **Figure 1** and **Figure 2** correspond to the solution of the tangential dipole radiation problem.

Eigenvalues $\Lambda_n^{(1)}$ and $\Lambda_n^{(2)}$ for the low-frequency breakdown behavior are also shown in **Figure 3**. One can observe that eigenvalues $\Lambda_n^{(1)}$ for SVS-EFIE-J formulation tend to infinity at low frequency, whereas $\Lambda_n^{(1)}$ with SVS-EFIE-M formulation is stable at low frequency.

Moreover, eigenvalues $\Lambda_n^{(1)}$ and $\Lambda_n^{(2)}$ for the range of discretization order are also shown in **Figure 4**. One can observe that eigenvalues $\Lambda_n^{(1)}$ for SVS-EFIE-J formulation (Goni, 2023) [9] increase with the increasing of the discretization order and hence suffer from oversampling breakdown, whereas, for the present work with SVS-EFIE-M formulation, $\Lambda_n^{(1)}$ is almost constant after certain range of the discretization order.

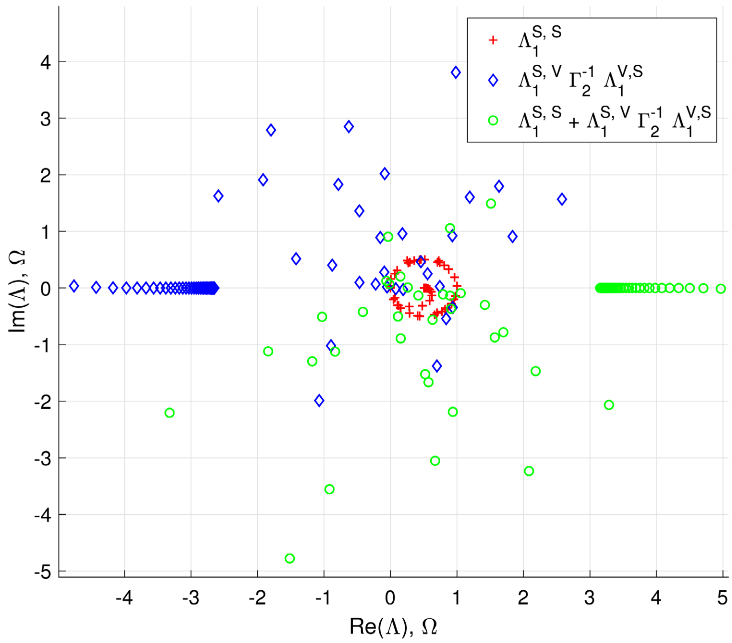

Figure 1. Eigenvalues $\Lambda^{S,S}_{1,m\epsilon,n}$ of the surface-to-surface operator, the product of eigenvalues $\Lambda^{S,V}_{1,e0,n}\hat{\Gamma}^{-1}_{2,n}\Lambda^{V,S}_{1,m\epsilon,n}$ corresponding to the product of the surface-to-volume and volume-to-surface operators and eigenvalues for the total SVS-EFIE-M operator $\Lambda^{(1)}_{n} = \Lambda^{S,S}_{1,m\epsilon,n} + \Lambda^{S,V}_{1e0,n}\hat{\Gamma}^{-1}_{1,n}\Lambda^{V,S}_{1,m\epsilon,n}$. One can observe the accumulation of those eigenvalues $\Lambda^{S,S}_{1,m\epsilon,n}$, $\Lambda^{S,V}_{1,e0,n}\hat{\Gamma}^{-1}_{2,n}\Lambda^{V,S}_{1,m\epsilon,n}$ and $\Lambda^{(1)}_{n}$ at constant values. We can also notice the behavior of the eigenvalues of surface-to-surface operator $\Lambda^{S,S}_{1,m\epsilon,n}$ encompassing a unit circle with centre at a constant of −1/2, which occurs due to their $-(1/2+\lambda_n)$ form stemming from the "constant + compact" operator composition [7].

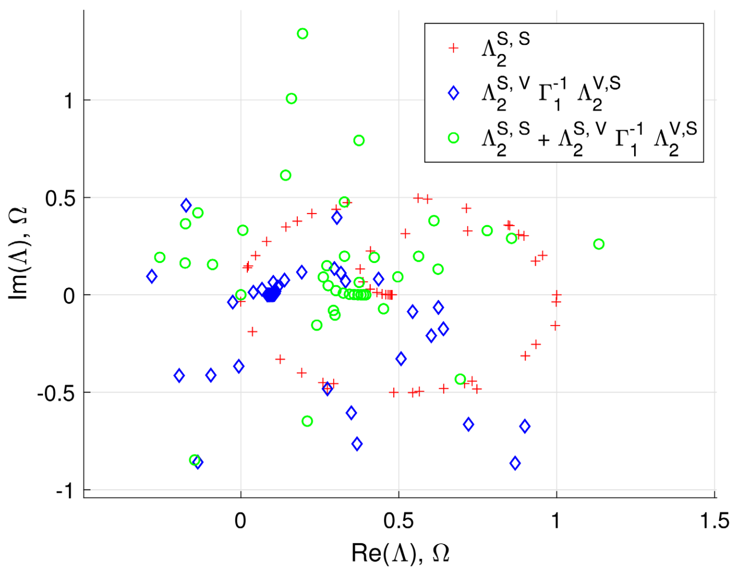

Figure 2. Eigenvalues $\Lambda^{S,S}_{2,m\epsilon,n}$ of the surface-to-surface operator, the product of eigenvalues $\Lambda^{S,V}_{2,e0,n}\hat{\Gamma}^{-1}_{1,n}\Lambda^{V,S}_{2,m\epsilon,n}$ corresponding to the product of the surface-to-volume and volume-to-surface operators, and eigenvalues $\Lambda^{(2)}_{n} = \Lambda^{S,S}_{2,m\epsilon,n} + \Lambda^{S,V}_{2e0,n}\hat{\Gamma}^{-1}_{1,n}\Lambda^{V,S}_{2,m\epsilon,n}$ for the total SVS-EFIE-M operator. One can observe the accumulation at constant values for all three sets of eigenvalues: $\Lambda^{S,S}_{2,m\epsilon,n}$, $\Lambda^{S,V}_{2,e0,n}\hat{\Gamma}^{-1}_{1,n}\Lambda^{V,S}_{2,m\epsilon,n}$ and $\Lambda^{(2)}_{n}$. We can also notice the behavior of the eigenvalues of surface-to-surface operator encompassing a unit circle centered at accumulation point of 1/2 due to the 'constant plus compact' operator structure, resulting in $\Lambda^{S,S}_{2,m\epsilon,n} = 1/2 - \lambda_n$ [7].

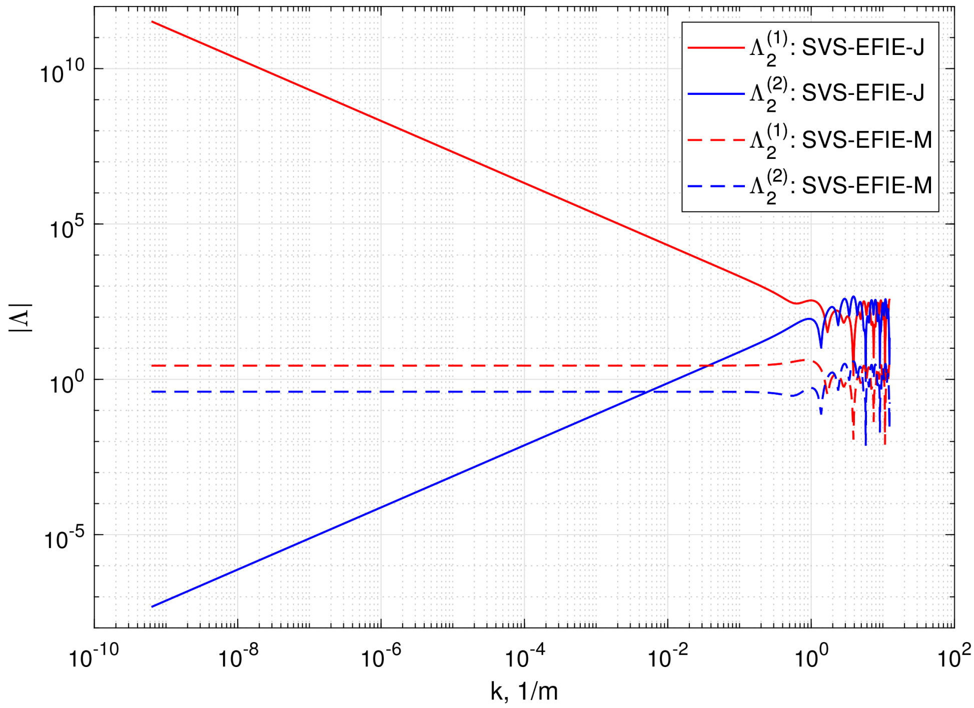

Figure 3. Eigenvalues $\Lambda_n^{(1)}$ and $\Lambda_n^{(2)}$ for the low-frequency breakdown. Notice that solid lines for the SVS-EFIE-J formulations and dashed lines correspond to SVS-EFIE-M formulations. One can observe that eigenvalues $\Lambda_n^{(1)}$ for J formulation tend to be infinite at low frequency, whereas $\Lambda_n^{(1)}$ is stable at low frequency.

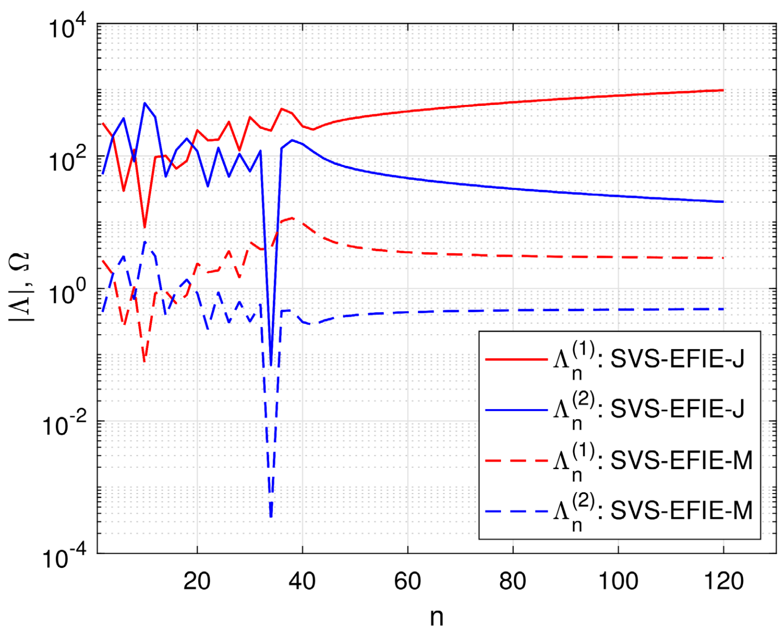

Figure 4. Eigenvalues $\Lambda_n^{(1)}$ and $\Lambda_n^{(2)}$ for the range of discretization order. Solid lines dictate SVS-EFIE-J formulations and dashed lines correspond to SVS-EFIE-M formulations. One can observe that eigenvalues $\Lambda_n^{(1)}$ for SVS-EFIE-J formulation increase with the increasing of the discretization order and hence suffer from oversampling breakdown, whereas, $\Lambda_n^{(1)}$ is almost constant after certain range of the discretization order.

6. Conclusion

The paper presents an analytic solution of the Surface-Volume-Surface Electric Field Integral Equations (SVS-EFIE) with Galerkin Method of Moments (MoM) for the problem of scattering due to tangential electric dipole excited on a homogenous dielectric sphere. It is shown that in order for the MoM impedance matrix condition number to remain bounded under the condition of increasing discretization order n, the SVS-EFIE-M can be tested in $L^2(S)$ space. This investigation also dictates that performing MoM solution in this $L^2(S)$ space can, in principle, eliminate the oversample breakdown and the low-frequency breakdown, unlike the SVS-EFIE-J. Note that alternative formulations such as PMCHWT, Muller, EFIE, MFIE, CFIE, and SVS-EFIE-J do not possess such desired spectral properties and suffer from the above breakdowns upon discretization.

Conflicts of Interest

The author declares no conflicts of interest regarding the publication of this paper.

References

[1] Hosseini Lori, F.S., Menshov, A., Gholami, R., Mojolagbe, J.B. and Okhmatovski, V.I. (2018) Novel Single-Source Surface Integral Equation for Scattering Problems by 3-D Dielectric Objects. *IEEE Transactions on Antennas and Propagation*, **66**, 797-807. https://doi.org/10.1109/tap.2017.2781740

[2] Menshov, A. and Okhmatovski, V. (2012) Novel Surface Integral Equation Formulation for Accurate Broadband RL Extraction in Transmission Lines of Arbitrary Cross-Section. 2012 *IEEE/MTT-S International Microwave Symposium Digest*, Montreal, 17-22 June 2012, 1-3. https://doi.org/10.1109/mwsym.2012.6259361

[3] Knockaert, L. and De Zutter, D. (1986) Integral Equation for the Fields Inside a Dielectric Cylinder Immersed in an incident E-Wave. *IEEE Transactions on Antennas and Propagation*, **34**, 1065-1067. https://doi.org/10.1109/tap.1986.1143940

[4] Swatek, D. (1999) Investigation of Single Source Surface Integral Equation for Electromagnetic Wave Scattering by Dielectric Bodies. Ph.D. Dissertation, The University of Manitoba. http://hdl.handle.net/1993/1699

[5] Kleinman, R.E. and Martin, P.A. (1988) On Single Integral Equations for the Transmission Problem of Acoustics. *SIAM Journal on Applied Mathematics*, **48**, 307-325. https://doi.org/10.1137/0148016

[6] Chew, W.C. (1999) Waves and Fields in Inhomogenous Media. Wiley-IEEE Press.

[7] Hsiao, G.C. and Kleinman, R.E. (1997) Mathematical Foundations for Error Estimation in Numerical Solutions of Integral Equations in Electromagnetics. *IEEE Transactions on Antennas and Propagation*, **45**, 316-328. https://doi.org/10.1109/8.558648

[8] Bloomfield, J.K., Face, S.H.P. and Moss, Z. (2017) Indefinite Integrals of Spherical Bessel Functions. arXiv: 1703.06428.

[9] Goni, O. (2023) Exact Solution of Surface-Volume-Surface Electric Field Integral Equation and Analysis of Its Spectral Properties. Ph.D. Dissertation, The University of Manitoba. https://mspace.lib.umanitoba.ca/server/api/core/bitstreams/d5dfa326-1389-421d-bac4-c463f53d6416/content

[10] Goni, O. and Okhmatovski, V.I. (2021) Analytic Solution of Surface-Volume-Surface Electric Field Integral Equation on Dielectric Sphere and Analysis of Its Spectral Properties. *IEEE Transactions on Antennas and Propagation*, **69**, 8479-8493. https://doi.org/10.1109/tap.2021.3083829

[11] Jones, D.S. (1989) Acoustic and Electromagnetic Waves. Oxford University Press.